Research article

An efficient spline technique for solving time-fractional integro-differential equations

Muhammad Abbas [a,*], Sadia Aslam [a], Farah Aini Abdullah [b],
Muhammad Bilal Riaz [c,d,e,**], Khaled A. Gepreel [f]

[a] *Department of Mathematics, University of Sargodha, Sargodha 40100, Pakistan*
[b] *School of Mathematical Sciences, Universiti Sains Malaysia, 11800 Penang, Malaysia*
[c] *Department of Computer Science and Mathematics, Lebanese American University, Byblos, Lebanon*
[d] *Faculty of Applied Physics and Mathematics, Gdańsk University of Technology, Narutowicza, 11/1280-233 Gdańsk, Poland*
[e] *Department of Mathematics, University of Management and Technology, 54770 C-II Johar Town Lahore, Pakistan*
[f] *Department of Mathematics and Statistics, College of Science, Taif University, P. O. Box 11099, Taif 21944, Saudi Arabia*

ARTICLE INFO

ABSTRACT

Spline curves are very prominent in the mathematics due to their simple construction, accuracy of assessment and ability to approximate complicated structures into interactive curved designs. A spline is a smooth piece-wise polynomial function. The primary goal of this study is to use extended cubic B-spline (ExCuBS) functions with a new second order derivative approximation to obtain the numerical solution of the weakly singular kernel (SK) non-linear fractional partial integro-differential equation (FPIDE). The spatial and temporal fractional derivatives are discretized by ExCuBS and the Caputo finite difference scheme, respectively. The present study found that it is stable and convergent. The validity of the current approach is examined on a few test problems, and the obtained outcomes are compared with those that have previously been reported in the literature.

1. Introduction

Splines are generally considered in dominant class of mathematical functions that are commonly utilized for estimation. A piece-wise polynomial function is referred to as a spline. For numerical interpretation of ODEs, PDEs and FPIDEs, the approximation scheme for spline functions have been frequently used. The more generic class of classical mechanics is fractional calculus. The concept of differentiation and integration to non-integral values has been investigated by fractional calculus. A number of applications of FDEs are investigated in finance, physics, engineering and seismology [1–3]. The integro-differential operator which covers both integer-order derivatives and integrals as special cases, is one of the reason why fractional calculus has grown so popular in recent years and has so many implementations [4]. General theory of heat conduction is applicable for nonlinear materials with memory and finite propagation speeds [5]. Dynamics of nuclear reactors [6], biofluids flow in fractured biomaterials [7], quadratic hedging problem [8], modeling dynamic fractional order viscoelasticity [9], population dynamics, convection diffusion [10] and grain growth [11] are examples of mathematical models of physical phenomenon and their applications. Some methods for solving FPIDEs because

---

they are a relatively new area of mathematics. These methods include the Adomian decomposition method [12,13], the fractional differential transform method [14], and the homotopy perturbation method [15,16].

In this paper, we will use an efficient spline technique to solve non-linear FPIDE with weakly SK. To discretize the time and space derivatives, the Caputo fractional derivative (CFD) approximation and new ExCuBS approximation for second derivative are applied, respectively. The non-linear FPIDE [30]

$$
{}_0^C D_t^\beta w(r,t) + w w_r = \int_0^t (t-\xi)^{\gamma-1} w_{rr}(r,\xi)d\xi + H(r,t), \qquad r \in [0,L], t \in [0,T], \tag{1}
$$

with initial condition (IC):

$$
w(r,0) = g(r), \quad r \in [0,L], \tag{2}
$$

and the boundary conditions (BCs):

$$
w(0,t) = w(L,t) = 0, \quad t \in [0,T], \tag{3}
$$

where $0 < \beta, \gamma < 1$ are fractional parameters, T, $L > 0$ are any constants and $H(r,t)$, $g(r)$ are given functions. The ${}_0^C D_t^\beta$ represents the CFD with Euler's Gamma function Γ, which is defined as:

$$
{}_0^C D_t^\beta w(r,t) = \begin{cases} \frac{1}{\Gamma(k-\beta)} \int_0^t \frac{\partial w(r,\mu)}{\partial \mu} \frac{d\mu}{(t-\mu)^{\beta-k+1}}, & k-1 < \beta \leq k, \quad k \in \mathbb{N}, \\ \frac{\partial^k w(r,t)}{\partial t^k}, & \beta = k. \end{cases}
$$

Non-integer order derivatives and operators in terms of integral are more appropriate than ordinary derivatives and integration at various phases of real systems because they give a more detailed explanation of the structural and genetic characteristics of a number of dynamical and physical processes. Because of this, precise computational methods are utilized to substantially handle the complexity of non-integer order derivatives present in such equations. These difficulties result from the potential for the kernel singularities to cause significant oscillations in the solution. Consequently, an approximation of the physical description is required because it is difficult to obtain a solution in closed form in many implementations, especially in nonlinear cases. As an alternative, numerous studies [17–19] have been carried out to determine a unique solution whether there is a singular solution to fractional order integro-differential equations. For simulating issues in engineering, mathematics biology, and other fields, the FPIDEs with weakly singular kernel are used. Due to weakly SK, it is very hard to find exact solutions of such problems, it is critical to achieve a numerical solution by utilizing various numerical approaches.

Uniqueness and existence findings for the solution of FPIDEs had made on a local and global scale in [20,21], respectively. Momani [22] has proposed local and global uniqueness theorems for solutions to non-integer order nonlinear differential equations. For a type of moderately SK Volterra integral equations, Diogo and Lima [23,24] have identified the discrete fast convergence of spline collocation techniques. In [25], high-order computational techniques are used to create and analyze problems with initial values for linear Volterra integro-differential equations with various types of discontinuities. For the solution of FPIDEs with weakly SKs, Nemati, et al. [26] has a scheme generated by matrices of Chebyshev polynomials. The operational matrix of fractional integration and the product have been used to convert the given equation into the solution of a system of linear algebraic equations. For the numerical solution of a class of nonlinear FPIDEs with weakly SKs, Nemati and Lima [27] have been considered the modification of hat functions. The operational matrix of fractional order for integration has been presented. Wang and Zhu [28] have presented a numerical technique for solving a variety of FPIDEs with a weakly SK that makes use of the 2nd Chebyshev wavelets operational matrix of non-integer order integration. The weakly singular FPIDEs are converted into an algebraic equation system by applying the operational matrix. An operational strategy based on the shifted Jacobi polynomials has been proposed by Biazar and Sadri [29] to obtain the solution of a type of weakly singular FPIDEs. The Caputo sense has been referred to as the fractional derivative operators. In order to approximate the SKs of this class of functional equations, a new operational matrix in addition to those for integration and product has been developed.

Akram et al. [30] solved the FPIDE by employing the ExCBS with the help of Caputo approach. They analyzed the stability and convergence to support the solutions. The authors used the classical approximation for the ExCBS functions and their derivatives. In present paper, we use the new approximation of second derivative which provides the more accuracy in numerical solution than the classical approximation. Awawdeh et al. [31] analytically solved the linear FPIDE by using the homotopy analysis approximation. Rawashdeh [32] proposed collocation approach to solve the FPIDE by using the spline presented in polynomial form. To deal with FPIDEs with weakly SKs, Zhao et al. [33] utilized collocation methods having piecewise polynomial form. By using a computational approach, Moghaddam and Machado [34] tried to interpret a variety of variable-order FIDEs with weakly SKs. In the correction functional, the CFD was estimated by an integer-order partial derivative by using the Variational Iteration Method [35].

A number of numerical algorithms to solve FPDEs have already been established. Nonlinear FPEs have been extensively used in finding numerical solutions by using diverse methods, it is consistent with the rapid development in finding the solutions to diverse problems stemming from the basic sciences. To solve fractional partial differential (FPD) models, many authors have developed the B-spline method [36–39]. Fairweather [40] suggested spline collocation techniques for the spatial quantization of a class of hyperbolic PIDEs. These functions can modify each point on the interval to get a close estimation of the optimal solution. Long et al. [41] proposed Tikhonov regularization method for finding an inverse source term in a fractional pseudo-parabolic equation. Long

et al. [42] investigated a global uniqueness and existence of solution of non-linear fractional diffusion involving Riemann–Liouville derivative. Ngoc et al. [43] considered boundary value problems for time-space fractional pseudo-parabolic equation with some boundary conditions. They investigated the continuity of the integral solution in terms of non-integer order.

The present study is outlined as follows: The ExCuBS basis functions and new approximation of second order derivative are defined in section 2. In section 3, time discretization and methodology are demonstrated. In sections 4 and 5, the suggested scheme's stability and convergence are investigated. The experimental outcomes are presented in section 6. Lastly, the concluding remarks of the proposed method are presented in section 7.

2. Preliminaries

2.1. Extended cubic B-spline basis functions

The ExCuBS basis functions are given in this section, for numerical solutions of proposed problem. The research community has shown interest in the concept of B-spline functions (BSFs) for the numerical outcomes of linear and non-linear BVPs in science and engineering. They are suitable to shape analysis because of their significant curve features and qualities. In order to find the accurate piece-wise numerical outcomes at any knot in the region, the BSFs have been proven to be superior to the standard finite difference method. The BSF of different degrees are utilized to achieve the approximate solution of several differential equations.

Let r_j be an equally spaced partition of a finite domain for $j \in Z$ and the interval is divided into $\hat{K}$ equal parts at the edges as $r_j = r_0 + jh$, where h is the step size. The ExCuBS basis functions over the defined interval at r_j are defined as [44,45]:

$$E_j^*(r, \kappa) = \frac{1}{24h^4} \begin{cases} 4h(1-\kappa)(r-r_{j-2})^3 + 3\kappa(r-r_{j-2})^4, & r \in [r_{j-2}, r_{j-1}), \\ (4-\kappa)h^4 + 12h^3(r-r_{j-1}) + 6h^2(2+\kappa)(r-r_{j-1})^2 - 12h(r-r_{j-1})^3 - 3\kappa(r-r_{j-1})^4, & r \in [r_{j-1}, r_j), \\ (4-\kappa)h^4 + 12h^3(r_{j+1}-r) + 6h^2(2+\kappa)(r_{j+1}-r)^2 - 12h(r_{j+1}-r)^3 - 3\kappa(r_{j+1}-r)^4, & r \in [r_j, r_{j+1}), \\ 4h(1-\kappa)(r_{j+2}-r)^3 + 3\kappa(r_{j+2}-r)^4, & r \in [r_{j+1}, r_{j+2}), \\ 0 & \text{otherwise,} \end{cases} \tag{4}$$

where $j = -1, 0, 1, ..., \hat{K} + 1$, $\kappa \in [-8, 1]$ is a variation parameter and $r \in R$ is a variable. Some geometric properties like non-negativity, partition of unity, and C^2 continuity of cubic B-spline (CuBS) and ExCuBS for $\kappa \in [-8, 1]$ are identical. The CuBS basis functions can be calculated easily by using recursive formula [46]. The ExCuBS is an extension of CuBS because it becomes CuBS for $\kappa = 0$. Assume that the ExCuBS approximate to the problem (1)-(3) is $W(r, t)$, such that

$$W(r, t) = \sum_{j=-1}^{\hat{K}+1} \zeta_j(t) E_j^*(r, \kappa), \tag{5}$$

where $\zeta_j(t)$ are the control points and $E_j^*(r, \kappa)$ are the ExCBS functions.

At the knots r_j, using the ExCuBS functions (4), the estimation of $W(r, t)$ given in (5) with its first and second derivative can be written as:

$$\begin{cases} W_j = \rho_1 \zeta_{j-1}(t) + \rho_2 \zeta_j(t) + \rho_1 \zeta_{j+1}(t), \\ W_j' = -\rho_3 \zeta_{j-1}(t) + \rho_3 \zeta_{j+1}(t), \\ W_j'' = \rho_4 \zeta_{j-1}(t) + \rho_5 \zeta_j(t) + \rho_4 \zeta_{j+1}(t), \end{cases} \tag{6}$$

where $\rho_1 = \frac{4-\kappa}{24}$, $\rho_2 = \frac{8+\kappa}{12}$, $\rho_3 = \frac{1}{2h}$, $\rho_4 = \frac{2+\kappa}{2h^2}$, $\rho_5 = -\frac{2+\kappa}{2h^2}$.

2.2. New approximation for second order derivative

We shall use the following ExCuBS with second order derivative approximation [47]:

$$W_j'' = \frac{1}{24h^2} \begin{cases} 2(14-\kappa)\zeta_{-1} + 3(3\kappa-22)\zeta_0 + 8(7-2\kappa)\zeta_1 + 14(\kappa-2)\zeta_2 + 6(2-\kappa)\zeta_3 + (\kappa-2)\zeta_4, & j = 0 \\ (2-\kappa)\zeta_{j-2} + 4(4+\kappa)\zeta_{j-1} - 6(6+\kappa)\zeta_j + 4(4+\kappa)\zeta_{j+1} + (2-\kappa)\zeta_{j+2}, & j = 1, 1, ..., \hat{K}-1 \\ (\kappa-2)\zeta_{\hat{K}-4} + 6(2-\kappa)\zeta_{\hat{K}-3} + 14(\kappa-2)\zeta_{\hat{K}-2} + 8(7-2\kappa)\zeta_{\hat{K}-1} + 3(3\kappa-22)\zeta_{\hat{K}} + 2(14-\kappa)\zeta_{\hat{K}+1}, & j = \hat{K} \end{cases} \tag{7}$$

3. Description of the numerical technique

3.1. Temporal discretization

Let $t^m = m\tau^*$, $m = 0, 1, ..., M$, where $\tau^* = \frac{T}{M}$ is a time moving scale. In the form of finite difference scheme the CFD approximation can be defined as:

$$_0^C D_t^\beta W(r,t) = \frac{1}{\Gamma(2-\beta)} \sum_{l=0}^{m} \frac{W(r, t^{m-l+1}) - W(r, t^{m-l})}{(\tau^*)^\beta} a_l^\beta + A^{m+1},$$ (8)

where $a_l^\beta = \left((l+1)^{1-\beta} - (l)^{1-\beta}\right)$.

$$|A^{m+1}| \leq A_0 (\tau^*)^{2-\beta},$$

where A_0 is a constant. The integral term in equation (1) at $t = t^{m+1}$ can be interpreted as:

$$\int_0^t (t-\xi)^{\gamma-1} W_{rr}(r,\xi)d\xi = \int_0^{t^{m+1}} (t^{m+1}-\xi)^{\gamma-1} W_{rr}(r,\xi)d\xi,$$ (9)

$$= \int_0^{t^{m+1}} \xi^{\gamma-1} W_{rr}(r, t^{m+1}-\xi)d\xi,$$

$$= \sum_{l=0}^{m} \int_{t^l}^{t^{l+1}} \xi^{\gamma-1} W_{rr}(r, t^{m+1}-\xi)d\xi,$$

$$= \sum_{l=0}^{m} \int_{t^l}^{t^{l+1}} \xi^{\gamma-1} W_{rr}(r, t^{m-l+1})d\xi,$$

$$= \frac{(\tau^*)^\gamma}{\gamma} \sum_{l=0}^{m} W_{rr}(r, t^{m-l+1})[(l+1)^\gamma - l^\gamma],$$

$$= \frac{(\tau^*)^\gamma}{\gamma} \sum_{l=0}^{m} W_{rr}(r, t^{m-l+1}) a_l^\gamma,$$

where $a_l^\gamma = ((l+1)^\gamma - l^\gamma)$.

Lemma 3.1. *The $a_l's$ satisfy the following conditions [39]:*

1. $a_0^\beta = 1$, $a_0^\gamma = 1$.
2. $a_0^\beta > a_1^\beta > a_2^\beta > ... > a_l^\beta$ and $a_0^\gamma > a_1^\gamma > a_2^\gamma > ... > a_l^\gamma$, $a_l^\beta, a_l^\gamma \to 0$ as $l \to \infty$.
3. $a_l^\beta, a_l^\gamma > 0$ for $l = 0, 1, ..., m$.
4. $\sum_{l=0}^{m}(a_l^\beta - a_{l+1}^\beta) + a_{m+1}^\beta = (1 - a_1^\beta) + \sum_{l=1}^{m-1}(a_l^\beta - a_{l+1}^\beta) + a_m^\beta = 1$.
5. $\sum_{l=0}^{m} a_l^\gamma > 1$.

3.2. Computation of the methodology

By substituting (8) and (9) in (1), we can write it as:

$$\frac{(\tau^*)^{-\beta}}{\Gamma(2-\beta)} \sum_{l=0}^{m} a_l^\beta(W^{m-l+1} - W^{m-l}) + (WW_r)^{m+1} = \frac{(\tau^*)^\gamma}{\gamma} \sum_{l=0}^{m} W_{rr}^{m-l+1} a_l^\gamma + H^{m+1}.$$ (10)

Non-linear term is linearized [51] as:

$$(WW_r)^{m+1} = W^{m+1} W_r^m + W^m W_r^{m+1} - W^m W_r^m.$$ (11)

By employing (11) into (10), we obtain

$$\frac{(\tau^*)^{-\beta}}{\Gamma(2-\beta)} \sum_{l=0}^{m} a_l^\beta(W^{m-l+1} - W^{m-l}) + W^{m+1} W_{\check{z}}^m + W^m W_r^{m+1} - (WW_r)^m = \frac{(\tau^*)^\gamma}{\gamma} \sum_{l=0}^{m} W_{rr}^{m-l+1} a_l^\gamma + H^{m+1}.$$

By using relation (5) in the above equation, we get

$$\frac{(\tau^*)^{-\beta}}{\Gamma(2-\beta)} \sum_{l=0}^{m} a_l^\beta (\sum_{j=-1}^{\hat{K}+1} \zeta_j^{m-l+1} E_j^* - \sum_{j=-1}^{\hat{K}+1} \zeta_j^{m-l} E_j^* + \sum_{j=-1}^{\hat{K}+1} \zeta_j^{m+1} E_j^* \sum_{j=-1}^{\hat{K}+1} \zeta_j^m \dot{E}_j^*$$

$$+ \sum_{j=-1}^{\hat{K}+1} \zeta_j^m E_j^* \sum_{j=-1}^{\hat{K}+1} \zeta_j^{m+1} \dot{E}_j^* - \sum_{j=-1}^{\hat{K}+1} \zeta_j^m E_j^* \sum_{j=-1}^{\hat{K}+1} \zeta_j^m \dot{E}_j^* = \frac{(\tau^*)^\gamma}{\gamma} \sum_{l=0}^{m} a_l^\gamma [\sum_{j=-1}^{\hat{K}+1} \zeta_j^{m-l+1} \ddot{E}_j^*] + H^{m+1},$$

where $\dot{E}_j^*$ and $\ddot{E}_j^*$ are the first and second derivatives of ExCuBS basis functions respectively. By letting $s = (\tau^*)^\beta \Gamma(2-\beta)$, $s_1 = \frac{(\tau^*)^\gamma}{\gamma}$ and after some simplification in the above equation, we have

$$W^{m+1} + sW^m W_r^{m+1} + sW^{m+1} W_r^m - ss_1 a_0^\gamma W_{rr}^{m+1}) = a_m^\beta W^0 + sW^m W_r^m$$

$$+ \sum_{l=0}^{m-1} (a_l^\beta - a_{l+1}^\beta) W^{m-l} + ss_1 \sum_{l=0}^{m-1} a_{l+1}^\gamma W_{rr}^{m-l} + sH^{m+1}. \tag{12}$$

By plugging (6), and (7) for $j = 0, 1, ..., \hat{K}$ into equation (12), we get

for $j = 0$,

$$(\rho_1 \zeta_{-1}^{m+1} + \rho_2 \zeta_0^{m+1} + \rho_1 \zeta_1^{m+1}) + s(\rho_1 \zeta_{-1}^{m+1} + \rho_2 \zeta_0^{m+1} + \rho_1 \zeta_1^{m+1})(-\rho_3 \zeta_{-1}^m + \rho_3 \zeta_1^m)$$

$$+ s(\rho_1 \zeta_{-1}^m + \rho_2 \zeta_0^m + \rho_1 \zeta_1^m)(-\rho_3 \zeta_{-1}^{m+1} + \rho_3 \zeta_1^{m+1}) - \frac{ss_1}{24h^2}(2(14-\kappa)\zeta_{-1}^{m+1} + 3(3\kappa-22)\zeta_0^{m+1} + 8(7-2\kappa)\zeta_1^{m+1}$$

$$+ 14(\kappa-2)\zeta_2^{m+1} + 6(2-\kappa)\zeta_3^{m+1} + (\kappa-2)\zeta_4^{m+1}) = a_m^\beta(\rho_1 \zeta_{-1}^0 + \rho_2 \zeta_0^0 + \rho_1 \zeta_1^0) + s(\rho_1 \zeta_{-1}^m + \rho_2 \zeta_0^m + \rho_1 \zeta_1^m)(-\rho_3 \zeta_{-1}^m$$

$$+ \rho_3 \zeta_1^m) + \sum_{l=0}^{m-1} (a_l^\beta - a_{l+1}^\beta)(\rho_1 \zeta_{-1}^{m-l} + \rho_2 \zeta_0^{m-l} + \rho_1 \zeta_1^{m-l}) + \frac{ss_1}{24h^2} \sum_{l=0}^{m-1} b_{l+1}^\gamma (2(14-\kappa)\zeta_{-1}^{m-l} + 3(3\kappa-22)\zeta_0^{m-l}$$

$$+ 8(7-2\kappa)\zeta_1^{m-l} + 14(\kappa-2)\zeta_2^{m-l} + 6(2-\kappa)\zeta_3^{m-l} + (\kappa-2)\zeta_4^{m-l}) + sH^{m+1},$$

for $j = 1, 1, ..., \hat{K}-1$,

$$(\rho_1 \zeta_{j-1}^{m+1} + \rho_2 \zeta_j^{m+1} + \rho_1 \zeta_{j+1}^{m+1}) + s(\rho_1 \zeta_{j-1}^{m+1} + \rho_2 \zeta_j^m + \rho_1 \zeta_{j+1}^{m+1})(-\rho_3 \zeta_{j-1}^m + \rho_3 \zeta_{j+1}^m)$$

$$+ s(\rho_1 \zeta_{j-1}^m + \rho_2 \zeta_j^m + \rho_1 \zeta_{j+1}^m)(-\rho_3 \zeta_{j-1}^{m+1} + \rho_3 \zeta_{j+1}^{m+1}) - \frac{ss_1}{24h^2}((2-\kappa)\zeta_{j-2}^{m+1} + 4(4+\kappa)\zeta_{j-1}^{m+1} - 6(6+\kappa)\zeta_j^{m+1}$$

$$+ 4(4+\kappa)\zeta_{j+1}^{m+1} + (2-\kappa)\zeta_{j+2}^{m+1}) = a_m^\beta(\rho_1 \zeta_{j-1}^0 + \rho_2 \zeta_j^0 + \rho_1 \zeta_{j+1}^0) + s(\rho_1 \zeta_{j-1}^m + \rho_2 \zeta_j^m + \rho_1 \zeta_{j+11}^m)(-\rho_3 \zeta_{j-1}^m + \rho_3 \zeta_{j+1}^m)$$

$$+ \sum_{l=0}^{m-1} (a_l^\beta - a_{l+1}^\beta)(\rho_1 \zeta_{j-1}^{m-l} + \rho_2 \zeta_j^{m-l} + \rho_1 \zeta_{j+1}^{m-l}) + \frac{ss_1}{24h^2} \sum_{l=0}^{m-1} s_{l+1}^\gamma((2-\kappa)\zeta_{j-2}^{m-l} + 4(4+\kappa)\zeta_{j-1}^{m-l} - 6(6+\kappa)\zeta_j^{m-l}$$

$$+ 4(4+\kappa)\zeta_{j+1}^{m-l} + (2-\kappa)\zeta_{j+2}^{m-l}) + sH^{m+1}, \tag{13}$$

for $j = \hat{K}$,

$$(\rho_1 \zeta_{\hat{K}-1}^{m+1} + \rho_2 \zeta_{\hat{K}}^{m+1} + \rho_1 \zeta_{\hat{K}+1}^{m+1}) + s(\rho_1 \zeta_{\hat{K}-1}^{m+1} + \rho_2 \zeta_{\hat{K}}^{m+1} + \rho_1 \zeta_{\hat{K}+1}^{m+1})(-\rho_3 \zeta_{\hat{K}-1}^m + \rho_3 \zeta_{\hat{K}+1}^m)$$

$$+ s(\rho_1 \zeta_{\hat{K}-1}^m + \rho_2 \zeta_{\hat{K}}^m + \rho_1 \zeta_{\hat{K}+1}^m)(-\rho_3 \zeta_{\hat{K}-1}^{m+1} + \rho_3 \zeta_{\hat{K}+1}^{m+1}) - \frac{ss_1}{24h^2}((\kappa-2)\zeta_{\hat{K}-4}^{m+1} + 6(2-\kappa)\zeta_{\hat{K}-3}^{m+1}$$

$$+ 14(\kappa-2)\zeta_{\hat{K}-2}^{m+1} + 8(7-2\kappa)\zeta_{\hat{K}-1}^{m+1} + 3(3\kappa-22)\zeta_{\hat{K}}^{m+1} + 2(14-\kappa)\zeta_{\hat{K}+1}^{m+1}) = a_m^\beta(\rho_1 \zeta_{\hat{K}-1}^0 + \rho_2 \zeta_{\hat{K}}^0 + \rho_1 \zeta_{\hat{K}+1}^0)$$

$$+ s(\rho_1 \zeta_{\hat{K}-1}^m + \rho_2 \zeta_{\hat{K}}^m + \rho_1 \zeta_{\hat{K}+1}^m)(-\rho_3 \zeta_{\hat{K}-1}^m + \rho_3 \zeta_{\hat{K}+1}^m) + \sum_{l=0}^{m-1} (a_l^\beta - a_{l+1}^\beta)(\rho_1 \zeta_{\hat{K}-1}^{m-l} + \rho_2 \zeta_{\hat{K}}^{m-l} + \rho_1 \zeta_{\hat{K}+1}^{m-l})$$

$$+ \frac{ss_1}{24h^2} \sum_{l=0}^{m-1} a_{l+1}^\gamma((\kappa-2)\zeta_{\hat{K}-4}^{m-l} + 6(2-\kappa)\zeta_{\hat{K}-3}^{m-l} + 14(\kappa-2)\zeta_{\hat{K}-2}^{m-l} + 8(7-2\kappa)\zeta_{\hat{K}-1}^{m-l} + 3(3\kappa-22)\zeta_{\hat{K}}^{m-l}$$

$$+ 2(14-\kappa)\zeta_{\hat{K}+1}^{m-l}) + sH^{m+1}.$$

3.3. Initial vector ζ^0

To initiate the loop on (12), we use initial condition for its computation which is given as:

$$\begin{cases} W_0' = g'(r_0), \\ W_j^0 = g(r_j), \ j = 0, 1, ..., \hat{K}, \\ W_{\hat{K}}' = g'(r_{\hat{K}}). \end{cases} \tag{14}$$

The order of the system is $(\hat{K}+3) \times (\hat{K}+3)$. Matrix form of the system of equations (14) is:

$$H_1 \zeta^0 = H_2,$$

where,

$$H_1 = \begin{pmatrix} -\rho_3 & 0 & \rho_3 & 0 & \dots & \dots & 0 \\ \rho_1 & \rho_2 & \rho_1 & 0 & \dots & \dots & 0 \\ 0 & \rho_1 & \rho_2 & \rho_1 & \dots & \dots & 0 \\ \vdots & \dots & \ddots & \ddots & \ddots & \dots & \vdots \\ \vdots & \dots & \dots & \dots & \rho_1 & \rho_2 & \rho_1 \\ 0 & \dots & \dots & \dots & -\rho_3 & 0 & \rho_3 \end{pmatrix}$$

and $H_2 = [g_0'(r_0), g(r_0), ..., g(r_{\hat{K}}), g_0'(r_{\hat{K}})]^T$.

4. Stability analysis

In this study, proposed method's stability will be analyzed. Numerical error and stability of numerical scheme are strongly related. A neutrally stable scheme is one in which the errors don't change as the calculations proceed. The numerical method is deemed to stable if the errors ultimately diminish and damp out. On the other hand, a numerical method is said to unstable if the errors continue to increase over time. By using Von Neumann stability analysis, the stability of numerical methods can be researched. Stability for time-dependent problems ensures that the numerical approach always yields a bounded solution when the exact differential equation's solution is bounded.

Theorem 1. *The proposed scheme of FPIDE* (1)-(3)*, is stable without any condition.*

Proof. The stability of the existing scheme is evaluated by employing Neumann approach. In the form of Fourier series, assume the following difference expression:

$$\Psi_q^m = w(r_q, t^m) - W_q^m = \phi^m e^{iq\psi h}, \tag{15}$$

where $i = \sqrt{-1}$. ψ and h are the mode number and step size, respectively. By choosing a constant s_2 instead of w in equation (11) to make the nonlinear term $w w_r$ linear, we obtain the following equation by employing (15):

$$\Psi_q^{m+1} + ss_2(\Psi_r)_q^{m+1} - ss_1(\Psi_{rr})_q^{m+1} = a_m^\beta \Psi_q^0 + \sum_{l=0}^{m-1}(a_l^\beta - a_{l+1}^\beta)\Psi_q^{m+1} + ss_1 \sum_{l=0}^{m-1} a_l^\gamma (\Psi_{rr})_q^{m-l}.$$

By using Equation (13), we achieve

$$\phi^{m+1}(\rho_1 e^{i(q-1)\psi h} + \rho_2 e^{iq\psi h} + \rho_1 e^{i(q+1)\psi h}) + ss_2 \phi^{m+1}(-\rho_3 e^{i(q-1)\psi h} + \rho_3 e^{i(q+1)\psi h}) - \frac{ss_1 \phi^{m+1}}{24h^2}((2-\kappa)e^{i(q-2)\psi h}$$

$$+ 4(4+\kappa)e^{i(q-1)\psi h} - 6(6+\kappa)e^{iq\psi h} + 4(4+\kappa)e^{i(q+1)\psi h} + (2-\kappa)e^{i(q+2)\psi h}) = a_m^\beta \phi^0(\rho_1 e^{i(q-1)\psi h} + \rho_2 e^{iq\psi h}$$

$$+ \rho_1 e^{i(q+1)\psi h}) + \sum_{l=0}^{m-1}(a_l^\beta - a_{l+1}^\beta)(\rho_1 e^{i(q-1)\psi h} + \rho_2 e^{iq\psi h} + \rho_1 e^{i(q+1)\psi h})\phi^{m-l} + \frac{ss_1}{24h^2} \sum_{l=0}^{m-1} a_l^\gamma (2-\kappa)e^{i(q-2)\psi h}$$

$$+ 4(4+\kappa)e^{i(q-1)\psi h} - 6(6+\kappa)e^{iq\psi h} + 4(4+\kappa)e^{i(q+1)\psi h} + (2-\kappa)e^{i(q+2)\psi h})\phi^{m-l}.$$

After some simplification, applying the values of $\rho_q' s$, we obtain

$$\phi^{m+1}[\frac{4-\kappa}{24}e^{-i\psi h} + \frac{8+\kappa}{12} + \frac{4-\kappa}{24}e^{i\psi h} + ss_2(-\frac{1}{2h}e^{-i\psi h} + \frac{1}{2h}e^{i\psi h}) - \frac{ss_1}{24h^2}((2-\kappa)e^{-2i\psi h} + 4(4+\kappa)e^{-i\psi h}$$

$$- 6(6+\kappa) + 4(4+\kappa)e^{i\psi h} + (2-\kappa)e^{2i\psi h})] = a_m^\beta \phi^0(\frac{4-\kappa}{24}e^{-i\psi h} + \frac{8+\kappa}{12} + \frac{4-\kappa}{24}e^{i\psi h})$$

$$+ \sum_{l=0}^{m-1}(a_l^\beta - a_{l+1}^\beta)(\frac{4-\kappa}{24}e^{-i\psi h} + \frac{8+\kappa}{12} + \frac{4-\kappa}{24}e^{i\psi h})\phi^{m-l} + \frac{ss_1}{24h^2} \sum_{l=0}^{m-1} a_l^\gamma (2-\kappa)e^{-2i\psi h}$$

$$+ 4(4+\kappa)e^{-i\psi h} - 6(6+\kappa) + 4(4+\kappa)e^{i\psi h} + (2-\kappa)e^{2i\psi h})\phi^{m-l}.$$

Now, by using trigonometric form of exponential function in the above equation and after some computation, we achieve

$$[\frac{8+\kappa}{12} + \frac{4-\kappa}{12}\cos\psi h + \frac{2ss_2}{2h}i\sin\psi h - \frac{ss_1(2-\kappa)}{12h^2}\cos 2\psi h - \frac{4ss_1(4+\kappa)}{12h^2}\cos\psi h + \frac{3ss_1(6+\kappa)}{12h^2}]\phi^{m+1}$$

$$= a_m^\beta \phi^0(\frac{8+\kappa}{12} + \frac{4-\kappa}{12}\cos\psi h) + \sum_{l=0}^{m-1}(a_l^\beta - a_{l+1}^\beta)(\frac{8+\kappa}{12} + \frac{4-\kappa}{12}\cos\psi h)\phi^{m-l}$$

$$+ \sum_{l=0}^{m-1} a_l^\gamma (\frac{ss_1(2-\kappa)}{12h^2}\cos 2\psi h + \frac{4ss_1(4+\kappa)}{12h^2}\cos\psi h - \frac{3ss_1(6+\kappa)}{12h^2})\phi^{m-l}.$$

We can write the above equation as:

$$(\alpha_1 + \alpha_2 + i\alpha_3)\phi^{m+1} = \alpha_1 a_m^\beta \phi^0 + \alpha_1 \sum_{l=0}^{m-1}(a_l^\beta - a_{l+1}^\beta)\phi^{m-l} - \alpha_2 \sum_{l=0}^{m-1} a_l^\gamma \phi^{m-l}, \tag{16}$$

where $\alpha_1 = \frac{8+\kappa}{12} + \frac{4-\kappa}{12}\cos\psi h$, $\alpha_2 = -\frac{ss_1(2-\kappa)}{12h^2}\cos 2\psi h - \frac{4ss_1(4+\kappa)}{12h^2}\cos\psi h + \frac{3ss_1(6+\kappa)}{12h^2}$, and $\alpha_3 = \frac{2ss_2}{2h} i \sin\psi h$.

From equation (16), we achieve

$$|\phi^{m+1}|^2 = \frac{[|\alpha_1(a_m^\beta \phi^0 + \sum_{l=0}^{m-1}(a_l^\beta - a_{l+1}^\beta)\phi^{m-l}) - \alpha_2 \sum_{l=0}^{m-1} a_l^\gamma \phi^{m-l}|]^2}{|(\alpha_1 + \alpha_2)^2 + (\alpha_3)^2|}. \tag{17}$$

For $m = 0$, equation (17) becomes:

$$|\phi^1|^2 = \frac{|\alpha_1 b_0^\beta \phi^0|^2}{|(\alpha_1 + \alpha_2)^2 + (\alpha_3)^2|} \leq |\phi^0|^2,$$

implies that

$$|\phi^1| \leq |\phi^0|.$$

Suppose that it is true for $|\phi^m| \leq |\phi^0|$, it must be satisfied for $|\phi^{m+1}|$. From (16), we have

$$(\alpha_1 + \alpha_2 + i\alpha_3)\phi^{m+1} = \alpha_1 a_m^\beta \phi^0 + \alpha_1 \sum_{l=0}^{m-1}(al^\beta - a_{l+1}^\beta)\phi^{m-l} - \alpha_2 \sum_{l=0}^{m-1} a_l^\gamma \phi^{m-l},$$

$$\leq \frac{\alpha_1 a_m^\beta \phi^0 + \alpha_1 \sum_{l=0}^{m-1}(a_l^\beta - a_{l+1}^\beta)\phi^{m-l}}{(\alpha_1 + \alpha_2 + i\alpha_3)},$$

$$|\phi^{m+1}| \leq \frac{|\alpha_1||a_m^\beta||\phi^0| + |\alpha_1|\sum_{l=0}^{m-1}(a_l^\beta - a_{l+1}^\beta)|\phi^{m-l}|}{\sqrt{(\alpha_1 + \alpha_2)^2 + (\alpha_3)^2}},$$

$$\leq \frac{|\alpha_1|}{\sqrt{(\alpha_1 + \alpha_2)^2 + (\alpha_3)^2}}[(a_0^\beta - a_1^\beta) + (a_1^\beta - a_2^\beta) + ... + (a_{m-1}^\beta - a_m^\beta)]|\phi^0|,$$

$$\leq |\phi^0|.$$

Thus, for each $m \geq 0$, we obtain

$$|\phi^{m+1}| \leq |\phi^0|. \tag{18}$$

From equations (15) and (18), we get

$$\Phi^{m+1} \leq \Phi^0, \ \forall m \geq 0.$$

Hence, the proposed technique for solving FPIDE is stable without any condition. □

5. Convergence analysis

In this part of study, we shall discuss the convergence of new ExCuBS estimation. We recall a few useful lemmas and theorems for this reason.

Lemma 5.1. *[36,48]. The ExCuBS basis set* $\{E_{-1}^*, E_0^*, ..., E_{\hat{K}+1}^*\}$ *defined in definition* (4) *holds the inequality*

$$\sum_{j=-1}^{\hat{K}+1} |E_j^*(r, \kappa)| \leq 1.75, \ 0 \leq r \leq 1.$$

Theorem 2. *[49,50]. Suppose that* $W(r_j, t) \in C^4[c, d], g \in C^2[c, d]$ *and* $\{r_j\}_{j \in Z}$ *be the equidistance partition of* $[c, d]$ *with step size h. There exists a constant* θ_i *free of h if the distinctive spline* $W(r, t)$ *that computes the ExCuBS solution, then, we get*

$$\|D^{\check{k}}(w(r, t) - W(r, t))\|_\infty \leq \theta_{\check{k}} h^{4-\check{k}}, \ \check{k} = 0, 1, 2, \ t \geq 0.$$

Theorem 3. *Let* $W(r, t)$ *be the approximate solution and* $w(r, t)$ *be the analytical solution of the FPIDE* (1)-(3) *exists. Moreover, if* $g \in C^2[0, 1]$, *then we have*

$$\|w(r, t) - W(r, t)\|_\infty \leq Sh^2,$$

where h is sufficiently small for every $t \geq 0$ *and* $S > 0$ *is free of h.*

Proof. Let $\hat{W}(r,t)$ be the computed spline to the estimated solution $w(r,t)$. By the use of triangular inequality, we get

$$\|w(r,t) - W(r,t)\|_\infty \le \|w(r,t) - \hat{W}(r,t)\|_\infty + \|\hat{W}(r,t) - W(r,t)\|_\infty. \tag{19}$$

By utilizing Theorem 2, we obtain

$$\|D^{\check{k}}(w(r,t) - W(r,t))\|_\infty \le \theta_{\check{k}} h^{4-\check{k}}, \ \check{k} = 0, 1, 2. \tag{20}$$

By using inequalities (19) and (20), the following expression is obtained:

$$\|w(r,t) - W(r,t)\|_\infty \le \theta_0 h^4 + \|\hat{W}(r,t) - W(r,t)\|_\infty. \tag{21}$$

By choosing a constant s_2 instead of w in equation (10) to make linear to nonlinear term ww_r, we obtain the following equation

$$W^{m+1} + sW^m W_r^{m+1} - ss_1 a_0^\gamma W_{rr}^{m+1}) = a_m^\beta W^0 + sW^m W_r^m + \sum_{l=0}^{m-1}(a_l^\beta - a_{l+1}^\beta)W^{m-l} + ss_1 \sum_{l=0}^{m-1} a_{l+1}^\gamma W_{rr}^{m-l} + sH^{m+1}.$$

The proposed scheme having collocation condition:

$$Lw(r_j,t) = LW(r_j,t) = H(r_j,t), \ j = 0, 1, ..., \hat{K}$$

Assume $LW(r_j,t) = \hat{H}(r_j,t)$. The difference expression "$L(\hat{W}(r_j,t) - W(r_j,t))$" of the current method at any time level m can be described as:

$$(\rho_1 \varepsilon_{j-1}^{m+1} + \rho_2 \varepsilon_j^{m+1} + \rho_1 \varepsilon_{j+1}^{m+1}) + ss_2(-\rho_3 \varepsilon_{j-1}^{m+1} + \rho_3 \varepsilon_{j+1}^{m+1}) - \frac{ss_1}{24h^2}((2-\kappa)\varepsilon_{j-2}^{m+1}$$
$$+ 4(4+\kappa)\varepsilon_{j-1}^{m+1} - 6(6+\kappa)\varepsilon_j^{m+1} + 4(4+\kappa)\varepsilon_{j+1}^{m+1} + (2-\kappa)\varepsilon_{j+2}^{m+1})$$
$$= a_m^\beta(\rho_1 \varepsilon_{j-1}^0 + \rho_2 \varepsilon_j^0 + \rho_1 \varepsilon_{j+1}^0) + \sum_{l=0}^{m-1}(a_l^\beta - a_{l+1}^\beta)(\rho_1 \varepsilon_{j-1}^{m-l} + \rho_2 \varepsilon_j^{m-l} + \rho_1 \varepsilon_{j+1}^{m-l}) \tag{22}$$
$$+ \frac{ss_1}{24h^2} \sum_{l=0}^{m-1} s_{l+1}^\gamma((2-\kappa)\varepsilon_{j-2}^{m-l} + 4(4+\kappa)\varepsilon_{j-1}^{m-l} - 6(6+\kappa)\varepsilon_j^{m-l} + 4(4+\kappa)\varepsilon_{j+1}^{m-l}$$
$$+ (2-\kappa)\varepsilon_{j+2}^{m-l}) + s[H^{m+1} - \hat{H}^{m+1}].$$

For $j = 0, \hat{K}$, we can write the following relations respectively:

$$(\rho_1 \varepsilon_{-1}^{m+1} + \rho_2 \varepsilon_0^{m+1} + \rho_1 \varepsilon_1^{m+1}) + ss_2(-\rho_3 \varepsilon_{-1}^{m+1} + \rho_3 \varepsilon_1^{m+1}) - \frac{ss_1}{24h^2}(2(14-\kappa)\varepsilon_{-1}^{m+1}$$
$$+ 3(3\kappa - 22)\varepsilon_0^{m+1} + 8(7-2\kappa)\varepsilon_1^{m+1} + 14(\kappa-2)\varepsilon_2^{m+1} + 6(2-\kappa)\varepsilon_3^{m+1} + (\kappa-2)\varepsilon_4^{m+1})$$
$$= a_m^\beta(\rho_1 \varepsilon_{-1}^0 + \rho_2 \varepsilon_0^0 + \rho_1 \varepsilon_1^0) + \sum_{l=0}^{m-1}(a_l^\beta - a_{l+1}^\beta)(\rho_1 \varepsilon_{-1}^{m-l} + \rho_2 \varepsilon_0^{m-l} + \rho_1 \varepsilon_1^{m-l}) \tag{23}$$
$$+ \frac{ss_1}{24h^2} \sum_{l=0}^{m-1} b_{l+1}^\gamma(2(14-\kappa)\varepsilon_{-1}^{m-1} + 3(3\kappa-22)\varepsilon_0^{m-1} + 8(7-2\kappa)\varepsilon_1^{m-1} + 14(\kappa-2)\varepsilon_2^{m-1}$$
$$+ 6(2-\kappa)\varepsilon_3^{m-1} + (\kappa-2)\varepsilon_4^{m-1}) + s[H^{m+1} - \hat{H}^{m+1}],$$

$$(\rho_1 \varepsilon_{\hat{K}-1}^{m+1} + \rho_2 \varepsilon_{\hat{K}}^{m+1} + \rho_1 \varepsilon_{\hat{K}+1}^{m+1}) + ss_2(-\rho_3 \varepsilon_{\hat{K}-1}^{m+1} + \rho_3 \varepsilon_{\hat{K}+1}^{m+1}) - \frac{ss_1}{24h^2}((\kappa-2)\varepsilon_{\hat{K}-4}^{m+1} + 6(2-\kappa)\varepsilon_{\hat{K}-3}^{m+1}$$
$$+ 14(\kappa-2)\varepsilon_{\hat{K}-2}^{m+1} + 8(7-2\kappa)\varepsilon_{\hat{K}-1}^{m+1} + 3(3\kappa-22)\varepsilon_{\hat{K}}^{m+1} + 2(14-\kappa)\varepsilon_{\hat{K}+1}^{m+1}) = a_m^\beta(\rho_1 \varepsilon_{\hat{K}-1}^0 + \rho_2 \varepsilon_{\hat{K}}^0$$
$$+ \rho_1 \varepsilon_{\hat{K}+1}^0) + \sum_{l=0}^{m-1}(a_l^\beta - a_{l+1}^\beta)(\rho_1 \varepsilon_{\hat{K}-1}^{m-l} + \rho_2 \varepsilon_{\hat{K}}^{m-l} + \rho_1 \varepsilon_{\hat{K}+1}^{m-l}) + \frac{ss_1}{24h^2} \sum_{l=0}^{m-1} a_{l+1}^\gamma((\kappa-2)\varepsilon_{\hat{K}-4}^{m-l} \tag{24}$$
$$+ 6(2-\kappa)\varepsilon_{\hat{K}-3}^{m-l} + 14(\kappa-2)\varepsilon_{\hat{K}-2}^{m-l} + 8(7-2\kappa)\varepsilon_{\hat{K}-1}^{m-l} + 3(3\kappa-22)\varepsilon_{\hat{K}}^{m-l} + 2(14-\kappa)\varepsilon_{\hat{K}+1}^{m-l})$$
$$+ s[H^{m+1} - \hat{H}^{m+1}].$$

For $j = 0, \hat{K}$, the following equations can be written by using BCs:

$$\rho_1 \varepsilon_{-1}^{m+1} + \rho_2 \varepsilon_0^{m+1} + \rho_1 \varepsilon_1^{m+1} = 0,$$
$$\rho_1 \varepsilon_{\hat{K}-1}^{m+1} + \rho_2 \varepsilon_{\hat{K}}^{m+1} + \rho_1 \varepsilon_{\hat{K}+1}^{m+1} = 0,$$

where,

$$\varepsilon_j^m = \zeta_j^m - \mu_j^m, \quad j = -1 : 1 : \hat{K}+1,$$

and

$$\Delta_j^m = h^2 |H_j^m - \hat{H}_j^m| \leq \theta h^4, \quad j = 0 : 1 : \hat{K}. \tag{25}$$

Assume that $\Delta^m = \max |\Delta_j^m|; 0 \leq j \leq \hat{K}$, $\epsilon_j^m = |\varepsilon_j^m|$ and $\epsilon^m = \max |\varepsilon_j^m|; 0 \leq j \leq \hat{K}$.

By choosing $m = 0$ in (22), we obtain

$$(\rho_1 \varepsilon_{j-1}^1 + \rho_2 \varepsilon_j^1 + \rho_1 \varepsilon_{j+1}^1) + ss_2(-\rho_3 \varepsilon_{j-1}^1 + \rho_3 \varepsilon_{j+1}^1) - \frac{ss_1}{24h^2}((2-\kappa)\varepsilon_{j-2}^1$$
$$+ 4(4+\kappa)\varepsilon_{j-1}^1 - 6(6+\kappa)\varepsilon_j^1 + 4(4+\kappa)\varepsilon_{j+1}^1 + (2-\kappa)\varepsilon_{j+2}^1)$$
$$= a_0^\beta(\rho_1 \varepsilon_{j-1}^0 + \rho_2 \varepsilon_j^0 + \rho_1 \varepsilon_{j+1}^0) + s[H^1 - \hat{H}^1], \quad j = 1 : 1 : \hat{K} - 1.$$

Now using equation (25), then taking absolute values of Δ_j^1, ε_j^1 and from IC, we get $\epsilon^0 = 0$. After some simplification and substituting values of $\rho' s$, the above relation can be written as:

$$\epsilon_j^1 \leq \frac{12s\theta h^4}{4h^2 - 6ss_1(6+\kappa)}, \quad j = 1 : 1 : \hat{K} - 1.$$

Substitute $m = 0$ in (23) to get

$$(\rho_1 \varepsilon_{-1}^1 + \rho_2 \varepsilon_0^1 + \rho_1 \varepsilon_1^1) + ss_2(-\rho_3 \varepsilon_{-1}^1 + \rho_3 \varepsilon_1^1) - \frac{ss_1}{24h^2}(2(14-\kappa)\varepsilon_{-1}^1 + 3(3\kappa - 22)\varepsilon_0^1 + 8(7-2\kappa)\varepsilon_1^1$$
$$+ 14(\kappa - 2)\varepsilon_2^1 + 6(2-\kappa)\varepsilon_3^1 + (\kappa - 2)\varepsilon_4^1) = a_m^\beta(\rho_1 \varepsilon_{-1}^0 + \rho_2 \varepsilon_0^0 + \rho_1 \varepsilon_1^0) + s[H^1 - \hat{H}^1].$$

By taking absolute values of Δ_0^1, ε_0^1, from IC, $\epsilon^0 = 0$ and then using values of $\rho' s$, we get

$$\epsilon_0^1 \leq \frac{12s\theta h^4}{4h^2 + 2ss_1(\kappa - 33)}.$$

Similarly, we can write for $j = N$ as:

$$\epsilon_{\hat{K}}^1 \leq \frac{12s\theta h^4}{4h^2 + 2ss_1(\kappa - 33)}.$$

By using BCs, we obtain

$$\epsilon_{-1}^1 \leq \theta h^2, \quad \epsilon_{\hat{K}+1}^1 \leq \theta h^2.$$

This gives,

$$\epsilon^1 \leq \theta_1 h^2,$$

where θ_1 is free of h.

By utilizing the induction technique, let $\epsilon_j^{\breve{q}}$ satisfy for $\breve{l} = 0 : 1 : \hat{K}$, and $\breve{q} = \max_{0 \leq l \leq m} \theta_l$, we have from (22)

$$[\frac{8+\kappa}{12} + \frac{6(6+\kappa)ss_1}{24h^2}]\varepsilon_j^{m+1} - \frac{(2-\kappa)ss_1}{24h^2}(\varepsilon_{j-2}^{m+1} + \varepsilon_{j+2}^{m+1}) + (\frac{4-\kappa}{24} - \frac{ss_2}{2h} - \frac{4(4+\kappa)ss_1}{24h^2})\varepsilon_{j-1}^{m+1}$$
$$+ (\frac{4-\kappa}{24} + \frac{ss_2}{2h} - \frac{4(4+\kappa)ss_1}{24h^2})\varepsilon_{j+1}^{m+1} = \sum_{l=0}^{m-1}(a_l^\beta - a_{l+1}^\beta)(\frac{4-\kappa}{24}\varepsilon_{j-1}^{m-l} + \frac{8+\kappa}{12}\varepsilon_j^{m-l} + \frac{4-\kappa}{24}\varepsilon_{j+1}^{m-l})$$
$$+ \frac{ss_1}{24h^2}\sum_{l=0}^{m-1}(a_{l+1}^\gamma((2-\kappa)\varepsilon_{j-2}^{m-l} + 4(4+\kappa)\varepsilon_{j-1}^{m-l} - 6(6+\kappa)\varepsilon_j^{m-l} + 4(4+\kappa)\varepsilon_{j+1}^{m-l}$$
$$+ (2-\kappa)\varepsilon_{j+2}^{m-l})) + s[H^{m+1} - \hat{H}^{m+1}].$$

By taking absolute values of Δ_j^{m+1} and ε_j^{m+1}, we obtain

$$\epsilon_j^{m+1} \leq \frac{12h^2}{4h^2 + 6ss_1(6+\kappa)}(\sum_{l=0}^{m-1}(a_l^\beta - a_{l+1}^\beta)\theta h^2 + s\theta_l h^2).$$

Similarly, by using BCs and equations (23) and (24), we get

$$\epsilon_0^{m+1} \leq \theta h^2, \quad \epsilon_{\hat{K}}^{m+1} \leq \theta h^2,$$
$$\epsilon_{-1}^{m+1} \leq \theta h^2, \quad \epsilon_{\hat{K}+1}^{m+1} \leq \theta h^2.$$

Hence for each value of m, $\exists$ a constant θ independent of h, therefore we have:

$$\epsilon^{m+1} \leq \theta h^2. \tag{26}$$

Now from (26) and Lemma 5.1, we get

$$\hat{W}(r,t) - W(r,t) = \sum_{j=-1}^{\hat{K}+1} (\zeta_j^m - \mu_j^m) E_j^*(r,\kappa).$$

Therefore,

$$\|\hat{W}(r,t) - W(r,t)\|_\infty \le 1.75\theta h^2.$$

Hence from above inequality and relation (21):

$$\|w(r,t) - W(r,t)\|_\infty \le \theta_0 h^4 + \|\hat{W}(r,t) - W(r,t)\|_\infty,$$

$$\le \theta_0 h^4 + 1.75\theta h^2 = Dh^2,$$

where $D = \theta_0 h^2 + 1.75\theta$. Hence $\exists$ a constant D free of h. $\quad\square$

6. Numerical experiments

To show the reliability of ExCuBS estimation for solving non-linear FPIDEs, two examples are demonstrated in this section. The computed outcomes are compared with [30]. The maximum error L_∞ and relative error L_2 are defined by:

$$L_\infty = \max_{0 \le j \le \hat{K}} |w(r_j,t) - W(r_j,t)|,$$

and

$$L_2 = \sqrt{\sum_{j=0}^{\hat{K}} |w(r_j,t) - W(r_j,t))|^2},$$

where $w(r,t)$ and $W(r,t)$ are exact and approximate solutions respectively.

To calculate order of convergence the following formula can be used [52]:

$$\breve{O} = \frac{log(L_\infty(\hat{K})) - log(L_\infty(\hat{K}+1))}{log(\hat{K}+1) - log(\hat{K})},$$

where $L_\infty(\hat{K})$ is the maximum errors at $\hat{K}$ and $L_\infty(\hat{K}+1)$ is the maximum errors at $\hat{K}+1$.

Example 6.1. The true problem given in equations (1)-(3) can be taken as:

$$_0^C D_t^\beta w(r,t) + ww_r = \int_0^t (t-\xi)^{\gamma-1} w_{rr}(r,\xi)d\xi + H(r,t),$$

with IC:

$$w(r,0) = r^2(1-r)^2,$$

where source term $H(r,t)$ is given as:

$$H(r,t) = \frac{\Gamma(\frac{7}{2})}{\Gamma(\frac{7}{2}-\beta)} t^{\frac{5}{2}-\beta} r^2(1-r)^2 - 2(\frac{1}{\gamma}t^\gamma + \frac{\Gamma(\frac{7}{2})\Gamma(\gamma)}{\Gamma(\frac{7}{2}+\gamma)} t^{\frac{5}{2}+\gamma})(1 - 6r + 6r^2) + 2(1 + t^{\frac{5}{2}})^2(1-2r)r^3(1-r)^3,$$

and exact solution is $w(r,t) = (1 + t^{\frac{5}{2}})r^2(1-r)^2$.

Table 1 represents the relative errors L_2 and absolute errors L_∞ computed by proposed scheme when $\beta = \frac{1}{4}, \frac{1}{2}$, $\gamma = 1.5 \times 10^{-1}$ at different values of τ^*. The comparison of the error norms L_2, L_∞ and convergence order with the results obtained by [30] is shown in Table 2 at various values of h. Absolute errors when $\gamma = 1.5 \times 10^{-1}$ at $T = 1$ for various β are tabulated in Table 3. In Fig. 1, we show the comparison of analytical and approximate solution for $\beta = \frac{1}{2}$, $\gamma = 0.01$, $\hat{K} = 50$ and $M = 100$ at $T = 1$. Fig. 2 illustrates the error graph at $\beta = \frac{3}{4}$, $\gamma = 0.15$ and $\hat{K} = M = 100$. Fig. 3(a) and Fig. 3(b) present the 3D plot for exact and approximate solutions when $\beta = \frac{1}{2}$, $\gamma = 0.05$, respectively. Fig. 4 shows the comparison of absolute errors for different values of β. Graphs illustrate the compatibility of analytical and computed solution. The advantage of proposed method is to provide a piecewise numerical solution at time $t = 1$ when other parameters are $\beta = \frac{3}{4}$, $\gamma = 0.15$, $\hat{K} = 20$ and $M = 100$.

Table 1

The L_∞, L_2 errors when $\gamma = 1.5 \times 10^{-1}$, $h = \frac{1}{1024}$ at T = 1 for Example 6.1.

| β	τ^*	ExCuBS [30]			Proposed method		
		L_2	L_∞	$\breve{O}$	L_2	L_∞	$\breve{O}$
1/4	1/4	1.02331×10^{-4}	5.06194×10^{-3}	...	2.11407×10^{-5}	9.56916×10^{-4}	...
1/4	1/8	3.19340×10^{-5}	1.50753×10^{-3}	1.74750	6.25900×10^{-6}	2.83664×10^{-4}	1.75421
1/4	1/16	8.54200×10^{-6}	4.45685×10^{-4}	1.75809	1.86431×10^{-6}	8.32160×10^{-5}	1.76931
1/4	1/32	1.88200×10^{-6}	1.33631×10^{-4}	1.73777	5.46132×10^{-7}	8.32512×10^{-5}	1.76864
1/2	1/4	1.02183×10^{-4}	5.05510×10^{-3}	...	2.11253×10^{-5}	8.13588×10^{-4}	...
1/2	1/8	3.19760×10^{-5}	1.51014×10^{-3}	1.74750	6.26233×10^{-6}	2.40874×10^{-4}	1.75602
1/2	1/16	8.17800×10^{-6}	4.55650×10^{-4}	1.72618	1.83705×10^{-6}	7.17469×10^{-5}	1.74729
1/2	1/32	1.95500×10^{-6}	1.34910×10^{-4}	1.75595	5.39147×10^{-7}	2.10176×10^{-5}	1.77132

Table 2

The L_∞, L_2 errors of Example 6.1, when $\gamma = 15 \times 10^{-2}$, $\tau^* = \frac{1}{1000}$, at T = 1.

β	h	ExCuBS [30]			Proposed method		
		L_2	L_∞	$\breve{O}$	L_2	L_∞	$\breve{O}$
1/2	1/4	1.82237×10^{-2}	5.49348×10^{-2}	...	3.07180×10^{-5}	1.07972×10^{-4}	...
1/2	1/8	3.45180×10^{-3}	1.36426×10^{-2}	2.00960	6.90725×10^{-6}	2.42786×10^{-5}	2.1529
1/2	1/16	7.83400×10^{-4}	3.31250×10^{-3}	2.04213	1.51007×10^{-6}	5.30780×10^{-6}	2.1935
1/2	1/32	2.50500×10^{-5}	8.01640×10^{-4}	2.04690	3.23158×10^{-7}	1.13588×10^{-6}	2.2243

$$w(r,1) = \begin{cases} 4.647 \times 10^{-16} + 7.229 \times 10^{-5}r + 1.983r^2 - 3.608r^3 - 1.704r^4, & r \in \left[0, \frac{1}{20}\right] \\ -8.224 \times 10^{-5} + 0.00493r + 1.889r^2 - 3.031r^3 - 1.166r^4, & r \in \left[\frac{1}{20}, \frac{1}{10}\right] \\ -6.175 \times 10^{-4} + 0.0205r + 1.743r^2 - 2.639r^3 - 0.687r^4, & r \in \left[\frac{1}{10}, \frac{3}{20}\right] \\ -0.002 + 0.048r + 1.577r^2 - 2.397r^3 - 0.269r^4, & r \in \left[\frac{3}{20}, \frac{1}{5}\right] \\ -0.004 + 0.086r + 1.414r^2 - 2.268r^3 + 0.089r^4, & r \in \left[\frac{1}{5}, \frac{1}{4}\right] \\ -0.009 + 0.133r + 1.263r^2 - 2.217r^3 + 0.388r^4, & r \in \left[\frac{1}{4}, \frac{3}{10}\right] \\ -0.015 + 0.187r + 1.126r^2 - 2.208r^3 + 0.628r^4, & r \in \left[\frac{3}{10}, \frac{7}{20}\right] \\ -0.023 + 0.250r + 0.991r^2 - 2.205r^3 + 0.807r^4, & r \in \left[\frac{7}{20}, \frac{2}{5}\right] \\ -0.034 + 0.327r + 0.837r^2 - 2.173r^3 + 0.927r^4, & r \in \left[\frac{2}{5}, \frac{9}{20}\right] \\ -0.051 + 0.430r + 0.631r^2 - 2.074r^3 + 0.987r^4, & r \in \left[\frac{9}{20}, \frac{1}{2}\right] \\ -0.076 + 0.581r + 0.330r^2 - 1.873r^3 + 0.987r^4, & r \in \left[\frac{1}{2}, \frac{11}{20}\right] \\ -0.115 + 0.808r - 0.118r^2 - 1.535r^3 + 0.927r^4, & r \in \left[\frac{11}{20}, \frac{3}{5}\right] \\ -0.179 + 1.153r - 0.780r^2 - 1.024r^3 + 0.807r^4, & r \in \left[\frac{3}{5}, \frac{13}{20}\right] \\ -0.281 + 1.673r - 1.731r^2 - 0.303r^3 + 0.628r^4, & r \in \left[\frac{13}{20}, \frac{7}{10}\right] \\ -0.440 + 2.436r - 3.056r^2 + 0.662r^3 + 0.388r^4, & r \in \left[\frac{7}{10}, \frac{3}{4}\right] \\ -0.682 + 3.531r - 4.853r^2 + 1.909r^3 + 0.089r^4, & r \in \left[\frac{3}{4}, \frac{4}{5}\right] \\ -1.042 + 5.065r - 7.229r^2 + 3.473r^3 - 0.269r^4, & r \in \left[\frac{4}{5}, \frac{17}{20}\right] \\ -1.564 + 7.163r - 10.302r^2 + 5.390r^3 - 0.687r^4, & r \in \left[\frac{17}{20}, \frac{9}{10}\right] \\ -2.303 + 9.976r - 14.203r^2 + 7.696r^3 - 1.166r^4, & r \in \left[\frac{9}{10}, \frac{19}{20}\right] \\ -3.329 + 13.676r - 19.070r^2 + 10.427r^3 - 1.704r^4, & r \in \left[\frac{19}{20}, 1\right] \end{cases}$$

Table 3
Absolute errors for Example 6.1 when $\gamma = 0.15$, at different values of r and β.

r/β	$\frac{1}{4}$	$\frac{1}{2}$	$\frac{3}{4}$	$\frac{19}{20}$
1/10	4.51176×10^{-5}	4.44825×10^{-5}	4.34865×10^{-5}	4.10961×10^{-5}
2/10	1.47802×10^{-4}	1.46566×10^{-4}	1.44627×10^{-4}	1.39971×10^{-4}
3/10	2.57386×10^{-4}	2.55647×10^{-4}	2.52917×10^{-4}	2.46362×10^{-4}
4/10	3.37822×10^{-4}	3.35747×10^{-4}	3.32487×10^{-4}	3.24657×10^{-4}
5/10	3.67407×10^{-4}	3.65211×10^{-4}	3.61763×10^{-4}	3.53478×10^{-4}
6/10	3.38715×10^{-4}	3.36634×10^{-4}	3.33368×10^{-4}	3.25520×10^{-4}
7/10	2.58720×10^{-4}	2.56974×10^{-4}	2.54234×10^{-4}	2.47650×10^{-4}
8/10	1.48983×10^{-4}	1.47740×10^{-4}	1.45790×10^{-4}	1.41108×10^{-4}
9/10	4.57573×10^{-5}	4.51182×10^{-5}	4.41164×10^{-5}	4.17108×10^{-5}
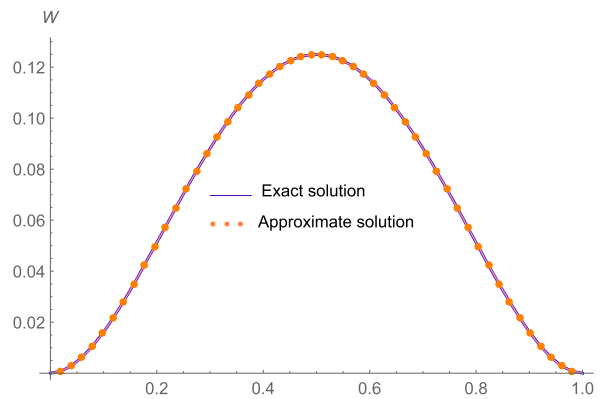
Fig. 1. Comparability of analytic and approximate solution when $\beta = \frac{1}{2}$ and $\gamma = 0.01$ for Example 6.1.
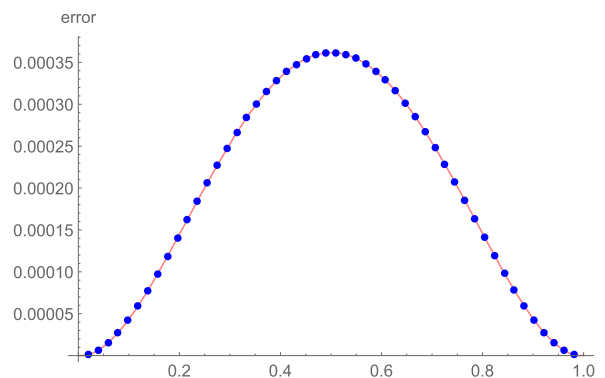
Fig. 2. Absolute errors graph when $\beta = \frac{3}{4}$ and $\gamma = 0.15$ for Example 6.1.

Example 6.2. Consider the non-linear FPIDE with initial condition

$$w(r,0) = \sin(\pi r),$$

and the source term $H(r,t)$ is:

$$H(r,t) = \pi(\frac{\pi}{\gamma} - 4t^3 \cos(2\pi r)) \sin(\pi r) + (\frac{\pi}{2} - \frac{12}{\Gamma(4-\beta)} t^{3-\beta} - 2\pi t^3 \cos(\pi r) - \frac{48\pi^2 \Gamma(\gamma)}{\Gamma(\gamma+4)} t^{3+\gamma}) \sin(2\pi r)$$

$$+ (8\pi t^6 \cos(2\pi r)) \sin(2\pi r).$$

The $w(r,t) = \sin(\pi r) - 2t^3 \sin(2\pi r)$ is true solution of proposed problem.

In Table 4, we show the comparison of L_2 calculated by proposed method with L_2 [30] for $\gamma = 0.15$, $\beta = \frac{1}{2}$, $\tau^* = 10^{-3}$ at various values of h. The absolute errors for various values of β, $\gamma = 0.05$, $h = \tau^* = 10^{-2}$ at different values of r are tabulated in Table 5.
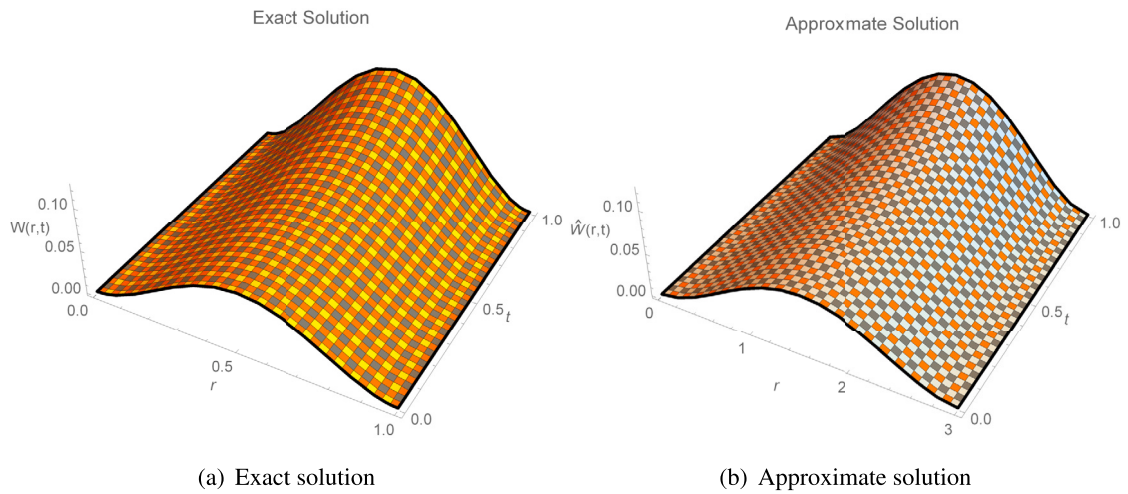
(a) Exact solution   (b) Approximate solution

Fig. 3. Comparison of 3D analytical and approximate solution when $\beta = \frac{1}{2}$ and $\gamma = 0.05$ for Example 6.1.
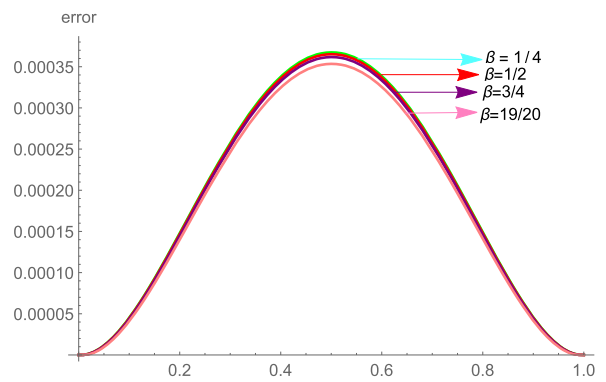

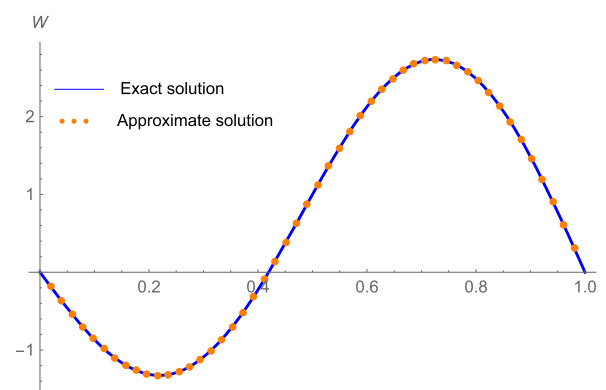**Fig. 4.** Comparability of absolute errors for Example 6.1 at different values of β.

Fig. 5. Comparability of exact and estimated solution at $\beta = \frac{1}{2}$ and $\gamma = 0.01$ for Example 6.2.

Fig. 5 presents the comparability of exact and estimated solution for $\beta = \frac{1}{2}$, $\gamma = 0.01$, $\hat{K} = 70$ and $M = 100$ at $T = 1$. Fig. 6 depicts the absolute error graph at $\beta = \frac{3}{4}$, $\gamma = 0.05$ and $\hat{K} = M = 100$. Fig. 7(a) and Fig. 7(b) depict the 3D plot for exact and numerical solutions at $\beta = \frac{1}{2}$, $\gamma = 0.15$, respectively. Fig. 8 reflects the comparability of absolute errors for some values of β. The advantage of proposed method is to provide a piecewise numerical solution at time $t = 1$ when other parameters are $\beta = 0.95$, $\gamma = 0.15$, $\hat{K} = 20$ and $M = 100$.
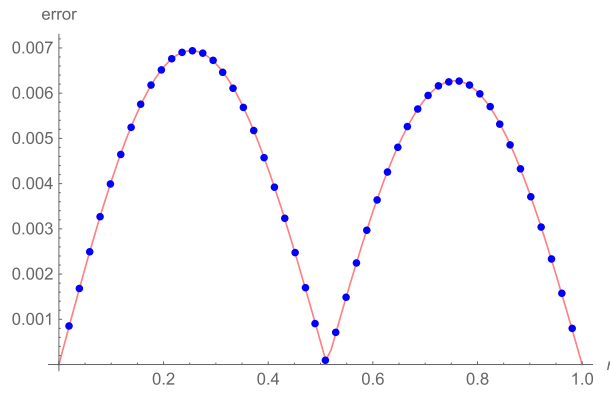
Fig. 6. Error graph of Example 6.2 when $\gamma = 5 \times 10^{-2}$.

(a) Exact solution

(b) Approximate solution

Fig. 7. Comparison of 3D analytical and approximate solution when $\beta = \frac{1}{2}$ and $\gamma = 0.15$ for Example 6.2.

Fig. 8. Comparability of absolute errors at different values of $\beta's$ for Example 6.2.

Table 4
The L_2 errors when $\gamma = 0.15$, $\tau^* = \frac{1}{1000}$, at $T = 1$ for Example 6.2.

β	h	ExCuBS [30]		Proposed method	
		L_2	$\breve{O}$	L_2	$\breve{O}$
1/2	1/4	2.219332×10^{-1}	...	6.78870×10^{-2}	...
1/2	1/8	4.56438×10^{-2}	1.489999	9.92961×10^{-3}	2.77333
1/2	1/16	5.87520×10^{-3}	1.495493	1.77884×10^{-3}	2.48080
1/2	1/32	6.88600×10^{-4}	1.497291	3.08178×10^{-4}	2.52910

$$w(r,1) = \begin{cases}
-2.722 \times 10^{-14} - 9.344r + 0.006r^2 + 114.435r^3 - 572.643r^4, & r \in \left[0, \frac{1}{20}\right] \\
-0.033 - 7.172r - 48.860r^2 + 548.753r^3 - 1657.974r^4, & r \in \left[\frac{1}{20}, \frac{1}{10}\right] \\
-0.537 + 8.848r - 227.383r^2 + 1326.932r^3 - 2573.486r^4, & r \in \left[\frac{1}{10}, \frac{3}{20}\right] \\
-2.771 + 55.719r - 569.115r^2 + 2281.388r^3 - 3223.658r^4, & r \in \left[\frac{3}{20}, \frac{1}{5}\right] \\
-8.543 + 144.829r - 1039.952r^2 + 3192.551r^3 - 3539.745r^4, & r \in \left[\frac{1}{5}, \frac{1}{4}\right] \\
-19.014 + 269.646r - 1532.493r^2 + 3822.368r^3 - 3485.936r^4, & r \in \left[\frac{1}{4}, \frac{3}{10}\right] \\
-32.788 + 395.969r - 1877.476r^2 + 3952.034r^3 - 3063.190r^4, & r \in \left[\frac{3}{10}, \frac{7}{20}\right] \\
-43.860 + 458.553r - 1871.593r^2 + 3418.736r^3 - 2309.338r^4, & r \in \left[\frac{7}{20}, \frac{2}{5}\right] \\
-40.285 + 366.854r - 1317.930r^2 + 2146.312r^3 - 1295.540r^4, & r \in \left[\frac{2}{5}, \frac{9}{20}\right] \\
-4.457 + 20.827r - 72.643r^2 + 165.347r^3 - 119.397r^4, & r \in \left[\frac{9}{20}, \frac{1}{2}\right] \\
84.280 - 664.603r + 1910.219r^2 - 2380.562r^3 + 1104.604r^4, & r \in \left[\frac{1}{2}, \frac{11}{20}\right] \\
244.491 - 1730.102r + 4544.298r^2 - 5243.900r^3 + 2256.356r^4, & r \in \left[\frac{11}{20}, \frac{3}{5}\right] \\
485.377 - 3143.108r + 7594.563r^2 - 8097.250r^3 + 3221.987r^4, & r \in \left[\frac{3}{5}, \frac{13}{20}\right] \\
798.586 - 4776.296r + 10684.408r^2 - 10569.860r^3 + 3905.121r^4, & r \in \left[\frac{13}{20}, \frac{7}{10}\right] \\
1150.885 - 6399.774r + 13328.315r^2 - 12292.651r^3 + 4236.398r^4, & r \in \left[\frac{7}{10}, \frac{3}{4}\right] \\
1479.866 - 7692.040r + 14988.240r^2 - 12946.268r^3 + 4180.313r^4, & r \in \left[\frac{3}{4}, \frac{4}{5}\right] \\
1694.828 - 8272.036r + 15147.957r^2 - 12306.220r^3 + 3738.690r^4, & r \in \left[\frac{4}{5}, \frac{17}{20}\right] \\
1684.411 - 7751.212r + 13396.264r^2 - 10279.329r^3 + 2950.483r^4, & r \in \left[\frac{17}{20}, \frac{9}{10}\right] \\
1331.519 - 5800.243r + 9507.052r^2 - 6926.138r^3 + 1887.848r^4, & r \in \left[\frac{9}{10}, \frac{19}{20}\right] \\
535.631 - 2225.515r + 3509.658r^2 - 2469.660r^3 + 649.886r^4, & r \in \left[\frac{19}{20}, 1\right]
\end{cases}$$

Example 6.3. Consider the non-linear FPIDE with initial condition

$$w(r,0) = \sin(\pi r),$$

and the source term $H(r,t)$ is:

$$H(r,t) = \frac{e^{-t}t^{2-\beta}\sin\pi r}{(2-\beta)\Gamma(2-\beta)} - \pi e^{-2t}\cos\pi r \sin\pi r + \frac{e^{-t}\pi^2 t^\gamma \sin\pi r}{\gamma}.$$

In Table 6, the approximate solutions for various values of β, $\gamma = 0.15$, $h = \tau^* = 10^{-2}$ at different values of r are tabulated. Fig. 9 illustrates the 2D plot for approximate solutions at $\beta = \frac{1}{2}$, $\gamma = 0.15$, $\hat{K} = M = 100$ at different time levels. Fig. 10 depicts the 3D plot for approximate solutions at $\beta = \frac{1}{2}$, $\gamma = 0.15$, $\hat{K} = M = 100$ at $T = 1$. The advantage of proposed method is to provide a piecewise numerical solution at time $t = 1$ when other parameters are $\beta = 0.75$, $\gamma = 0.001$, $\hat{K} = 20$ and $M = 100$.
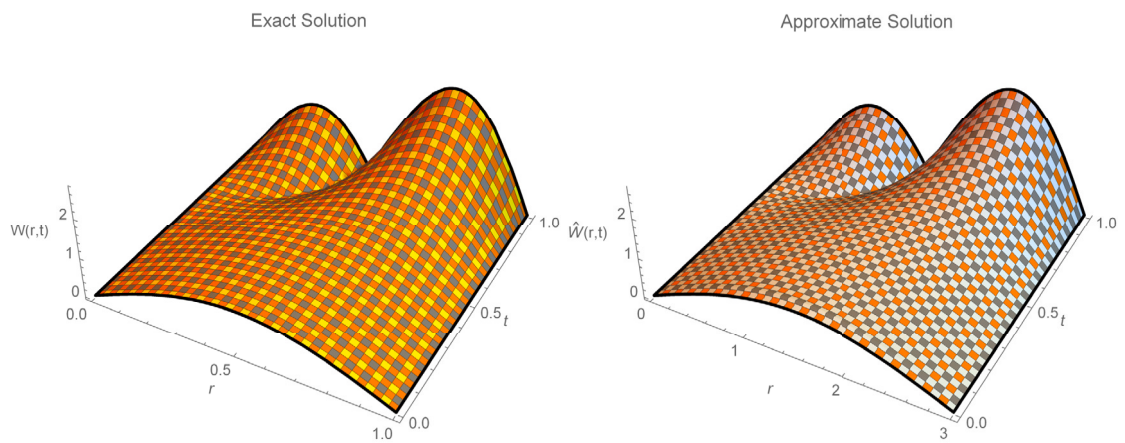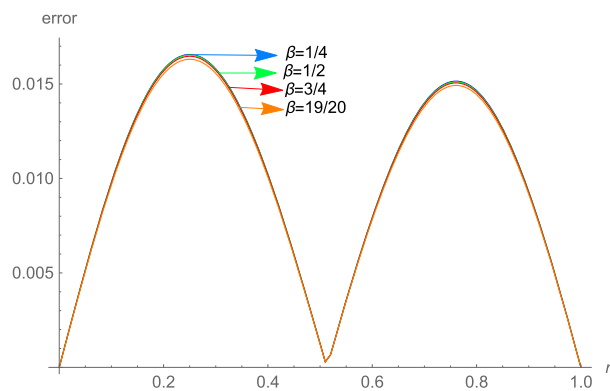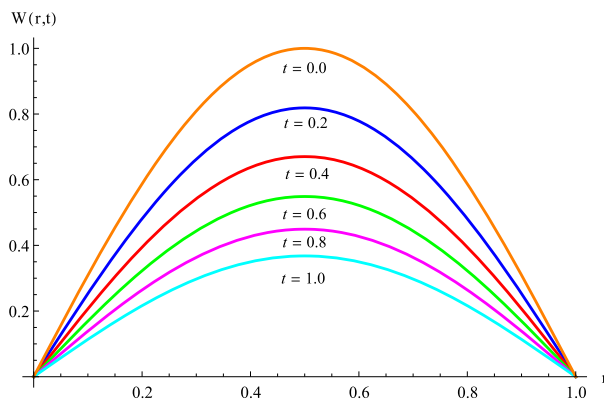
Table 5
Absolute errors when $\gamma = \frac{1}{20}$ at several values of r for Example 6.2.

r/β	$\frac{1}{4}$	$\frac{1}{2}$	$\frac{3}{4}$	$\frac{19}{20}$
1/10	4.05749×10^{-3}	4.0548×10^{-3}	4.04501×10^{-3}	4.01895×10^{-3}
2/10	6.25693×10^{-3}	6.57856×10^{-3}	6.56279×10^{-3}	6.52064×10^{-3}
3/10	6.65962×10^{-3}	6.6559×10^{-3}	6.64023×10^{-3}	6.5979×10^{-3}
4/10	4.31883×10^{-3}	4.31739×10^{-3}	4.30779×10^{-3}	4.28096×10^{-3}
5/10	4.78866×10^{-4}	4.80757×10^{-4}	4.80867×10^{-4}	4.79205×10^{-4}
6/10	3.4167×10^{-3}	3.41164×10^{-3}	3.4018×10^{-3}	3.37805×10^{-3}
7/10	5.91187×10^{-3}	5.90503×10^{-3}	5.88908×10^{-3}	5.84919×10^{-3}
8/10	6.05741×10^{-3}	6.05093×10^{-3}	6.03489×10^{-3}	5.99435×10^{-3}
9/10	3.78909×10^{-3}	3.78516×10^{-3}	3.7752×10^{-3}	3.74991×10^{-3}

Fig. 9. 2D approximate solution at $\beta = \frac{1}{2}$ and $\gamma = 0.15$ for Example 6.3.
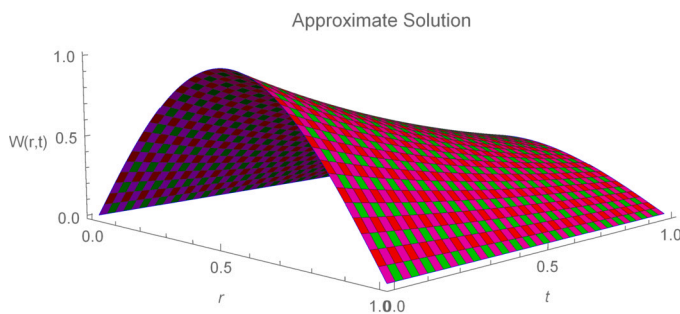
Fig. 10. 3D approximate solution at $\beta = \frac{1}{2}$ and $\gamma = 0.15$ for Example 6.3.

Table 6
Approximate solutions when $\gamma = 15 \times 10^{-2}$ at different values of r for Example 6.3.

r/β	$\frac{1}{4}$	$\frac{1}{2}$	$\frac{3}{4}$	$\frac{19}{20}$
1/10	9.75272×10^{-2}	9.73826×10^{-2}	9.69077×10^{-2}	9.62702×10^{-2}
2/10	1.885474×10^{-1}	1.85197×10^{-1}	1.84292×10^{-1}	1.83077×10^{-1}
3/10	2.55209×10^{-1}	2.54826×10^{-1}	2.53575×10^{-1}	2.51898×10^{-1}
4/10	2.99907×10^{-1}	2.99452×10^{-1}	2.97976×10^{-1}	2.95998×10^{-1}
5/10	3.15213×10^{-1}	3.14731×10^{-1}	3.1317×10^{-1}	3.11082×10^{-1}
6/10	2.99664×10^{-1}	2.99201×10^{-1}	2.97709×10^{-1}	2.95716×10^{-1}
7/10	2.54816×10^{-1}	2.54418×10^{-1}	2.53144×10^{-1}	2.51442×10^{-1}
8/10	1.8508×10^{-1}	1.8479×10^{-1}	1.83861×10^{-1}	1.82621×10^{-1}
9/10	9.72843×10^{-2}	9.71307×10^{-2}	9.66411×10^{-2}	9.59881×10^{-2}

$$w(r,1) = \begin{cases} -1.101 \times 10^{-15} + 1.154r - 0.00001r^2 - 1.894r^3 - 0.014r^4, & r \in \left[0, \frac{1}{20}\right] \\ -0.000006 + 1.1549r - 0.0082r^2 - 1.836r^3 - 0.042r^4, & r \in \left[\frac{1}{20}, \frac{1}{10}\right] \\ -0.0001 + 1.1581r - 0.040r^2 - 1.722r^3 - 0.069r^4, & r \in \left[\frac{1}{10}, \frac{3}{20}\right] \\ -0.0006 + 1.168r - 0.1126r^2 - 1.555r^3 - 0.094r^4, & r \in \left[\frac{3}{20}, \frac{1}{5}\right] \\ -0.002 + 1.193r - 0.236r^2 - 1.340r^3 - 0.117r^4, & r \in \left[\frac{1}{5}, \frac{1}{4}\right] \\ -0.006 + 1.238r - 0.421r^2 - 1.083r^3 - 0.137r^4, & r \in \left[\frac{1}{4}, \frac{3}{10}\right] \\ -0.013 + 1.313r - 0.673r^2 - 0.792r^3 - 0.154r^4, & r \in \left[\frac{3}{10}, \frac{7}{20}\right] \\ -0.026 + 1.425r - 0.996r^2 - 0.476r^3 - 0.167r^4, & r \in \left[\frac{7}{20}, \frac{2}{5}\right] \\ -0.047 + 1.580r - 1.386r^2 - 0.144r^3 - 0.176r^4, & r \in \left[\frac{2}{5}, \frac{9}{20}\right] \\ -0.077 + 1.782r - 1.837r^2 + 0.193r^3 - 0.180r^4, & r \in \left[\frac{9}{20}, \frac{1}{2}\right] \\ -0.119 + 2.033r - 2.339r^2 + 0.528r^3 - 0.180r^4, & r \in \left[\frac{1}{2}, \frac{11}{20}\right] \\ -0.173 + 2.330r - 2.8766r^2 + 0.849r^3 - 0.176r^4, & r \in \left[\frac{11}{20}, \frac{3}{5}\right] \\ -0.241 + 2.666r - 3.430r^2 + 1.146r^3 - 0.167r^4, & r \in \left[\frac{3}{5}, \frac{13}{20}\right] \\ -0.320 + 3.029r - 3.978r^2 + 1.410r^3 - 0.154r^4, & r \in \left[\frac{13}{20}, \frac{7}{10}\right] \\ -0.409 + 3.404r - 4.497r^2 + 1.634r^3 - 0.137r^4, & r \in \left[\frac{7}{10}, \frac{3}{4}\right] \\ -0.503 + 3.770r - 4.962r^2 + 1.810r^3 - 0.117r^4, & r \in \left[\frac{3}{4}, \frac{4}{5}\right] \\ -0.594 + 4.100r - 5.345r^2 + 1.933r^3 - 0.094r^4, & r \in \left[\frac{4}{5}, \frac{17}{20}\right] \\ -0.674 + 4.367r - 5.623r^2 + 1.999r^3 - 0.069r^4, & r \in \left[\frac{17}{20}, \frac{9}{10}\right] \\ -0.731 + 4.539r - 5.771r^2 + 2.005r^3 - 0.042r^4, & r \in \left[\frac{9}{10}, \frac{19}{20}\right] \\ -0.753 + 4.584r - 5.767r^2 + 1.951r^3 - 0.014r^4, & r \in \left[\frac{19}{20}, 1\right] \end{cases}$$

7. Conclusion

In this study, the ExCuBS has been used to find the numerical solution of non-linear FPIDEs. The CFD approximation based on finite difference and ExCuBS approach have been utilized to discretize time and spatial derivatives, respectively. This novel scheme has been equipped with new approximation of second order derivative of ExCuBS. The proposed technique has been tested by some numerical experiments. Also, the stability and convergence analysis of the proposed method have been analyzed. This novel approach has presented more accurate results than the numerical techniques found in existing literature due to its new approximation for second derivative of basis functions. In future, we can use Caputo-Fabrizio and Atangana-Baleanu fractional order derivative along with new approximation for higher order derivatives to get more accurate results.

CRediT authorship contribution statement

Muhammad Abbas, Sadia Aslam: Conceived and designed the experiments; Performed the experiments; Contributed reagents, materials, analysis tools or data; Wrote the paper. **Farah Aini Abdullah:** Conceived and designed the experiments; Analyzed and interpreted the data; Wrote the paper. **Muhammad Bilal Riaz:** Conceived and designed the experiments; Analyzed and interpreted the data. **Khaled A. Gepreel:** Conceived and designed the experiments; Performed the experiments; Analyzed and interpreted the data; Wrote the paper.

Declaration of competing interest

The authors declare no conflict of interest.

Data availability statement

No data was used for the research described in the article.

Acknowledgement

References

[1] C. Celik, M. Duman, Crank-Nicolson method for the fractional diffusion equation with the Riesz fractional derivative, J. Comput. Phys. 231 (4) (2012) 1743–1750.

[2] I.I. Gorial, Numerical methods for fractional reaction-dispersion equation with Riesz space fractional derivative, Eng. Technol. J 29 (4) (2011) 709–715.

[3] H. Jafari, V.D. Gejii, Solving linear and nonlinear fractional diffusion and wave equations by Adomian decomposition, Appl. Math. Comput. 180 (2) (2006) 488–497.

[4] T. Kisela, Fractional Differential Equations and Their Applications, Faculty of Mechanical Engineering Institute of Mathematics, 2008.

[5] M.E. Gurtin, A.C. Pipkin, A general theory of heat conduction with finite wave speeds, Arch. Ration. Mech. Anal. 31 (1968) 113–126.

[6] C.V. Pao, L. Payne, H. Amann, Bifurcation analysis of a nonlinear diffusion system in reactor dynamics, Appl. Anal. 9 (1977) 107–119.

[7] K.S. Zadeh, An integro-partial differential equation for modeling biofluids flow in fractured biomaterials, J. Theor. Biol. 273 (2011) 72–79.

[8] P. Hepperger, Hedging electricity swaptions using partial integro-differential equations, Stoch. Process. Appl. 122 (2012) 600–622.

[9] S. Larsson, M. Racheva, F. Saedpanah, Discontinuous Galerkin method for an integro-differential equation modeling dynamic fractional order viscoelasticity, Comput. Methods Appl. Mech. Eng. 283 (2015) 196–209.

[10] F. Mirzaee, S. Alipour, A hybrid approach of nonlinear partial mixed integro-differential equations of fractional order, Iran. J. Sci. Technol. Trans. A, Sci. 44 (2020) 725–737.

[11] F.S. Ng, Statistical mechanics of normal grain growth in one dimension: a partial integro-differential equation model, Acta Mater. 120 (2016) 453–462.

[12] S. Momani, R. Qaralleh, An efficient method for solving systems of fractional integro-differential equations, Comput. Math. Appl. 52 (3–4) (2006) 459–470.

[13] S. Momani, M.A. Noor, Numerical methods for fourth-order fractional integro-differential equations, Appl. Math. Comput. 182 (1) (2006) 754–760.

[14] A. Arikoglu, I. Ozkol, Solution of fractional integro-differential equations by using fractional differential transforms method, Chaos Solitons Fractals 40 (2) (2009) 521–529.

[15] S.H. Hosseinnia, A. Ranjbar, S. Momani, Using an enhanced homotopy perturbation method in fractional differential equations via deforming the linear part, Comput. Math. Appl. 56 (12) (2008) 3138–3149.

[16] R.K. Saeed, H.M. Sdeq, Solving a system of linear Fredholm fractional integro-differential equations using homotopy perturbation method, Aust. J. Basic Appl. Sci. 4 (4) (2010) 633–638.

[17] L. Hu, Y. Ren, R. Sakthivel, Existence and uniqueness of mild solutions for semilinear integro-differential equations of fractional order with nonlocal conditions, Semigroup Forum 79 (2009) 507–514.

[18] F. Li, J. Liang, H.K. Xu, Existence of mild solutions for fractional integro-differential equations of Sobolev type with nonlocal conditions, J. Math. Anal. Appl. 391 (2012) 510–525.

[19] K. Karthikeyan, J.J. Trujillo, Existence and uniqueness results for fractional integrodifferential equations with boundary value conditions, Commun. Nonlinear Sci. Numer. Simul. 17 (2012) 4037–4043.

[20] S.M. Monnani, Local and global existence theorems on fractional integro-differential equations, J. Fract. Calc. 18 (2000) 81–86.

[21] S. Momani, A. Jameel, S.O.R.A. Al-Azawi, Local and global uniqueness theorems on fractional integro-differential equations via Bihari's and Gronwall's inequalities, Soochow J. Math. 33 (4) (2007) 619.

[22] S.M. Momani, Local and global uniqueness theorems on differential equations of non-integer order via Bihari's and Gronwall's inequalities, Rev. Téc. Fac. Ing., Univ. Zulia 23 (1) (2000) 66–69.

[23] T. Diogo, P. Lima, Superconvergence of collocation methods for a class of weakly singular Volterra integral equations, J. Comput. Appl. Math. 218 (2) (2008) 307–316.

[24] T. Diogo, P. Lima, Collocation solutions of a weakly singular Volterra integral equation, Trends Comput. Appl. Math. 8 (2) (2007) 229–238.

[25] T. Diogo, P.M. Lima, A. Pedas, G. Vainikko, Smoothing transformation and spline collocation for weakly singular Volterra integro-differential equations, Appl. Numer. Math. 114 (2017) 63–76.

[26] S. Nemati, S. Sedaghat, I. Mohammadi, A fast numerical algorithm based on the second kind Chebyshev polynomials for fractional integro-differential equations with weakly singular kernels, J. Comput. Appl. Math. 308 (2016) 231–242.

[27] S. Nemati, P.M. Lima, Numerical solution of nonlinear fractional integro-differential equations with weakly singular kernels via a modification of hat functions, Appl. Math. Comput. 327 (2018) 79–92.

[28] Y. Wang, L. Zhu, SCW method for solving the fractional integro-differential equations with a weakly singular kernel, Appl. Math. Comput. 275 (2016) 72–80.

[29] J. Biazar, K. Sadri, Solution of weakly singular fractional integro-differential equations by using a new operational approach, J. Comput. Appl. Math. 352 (2019) 453–477.

[30] T. Akram, Z. Ali, F. Rabiei, K. Shah, P. Kumam, A numerical study of nonlinear fractional order partial integro-differential equation with a weakly singular kernel, Fractal Fract. 5 (2021) 85.

[31] H. Jaradat, F. Awawdeh, E. Rawashdeh, On Volterra's population growth models, An. Univ. Craiova, Math. Comput. Sci. Ser. 38 (2) (2011) 18–25.

[32] E. Rawashdeh, Numerical solution of fractional integro-differential equations by collocation method, Appl. Math. Comput. 176 (2006) 1–6.

[33] J. Zhao, J. Xiao, N.J. Ford, Collocation methods for fractional integro-differential equations with weakly singular kernels, Numer. Algorithms 65 (4) (2014) 723–743.

[34] B.P. Moghaddam, J.A. Tenreiro Machado, A computational approach for the solution of a class of variable-order fractional integro-differential equations with weakly singular kernels, Fract. Calc. Appl. Anal. 20 (4) (2017) 1023–1042.

[35] J.R. Loh, C. Phang, Numerical solution of Fredholm fractional integro-differential equation with right-sided Caputo's derivative using Bernoulli polynomials operational matrix of fractional derivative, J. Math. 16 (2) (2019) 1–25.

[36] S.T. Mohyud-Din, T. Akram, M. Abbas, A.I. Ismail, N.M. Ali, A fully implicit finite difference scheme based on extended cubic B-splines for time fractional advection-diffusion equation, Adv. Differ. Equ. 2018 (2018) 109.

[37] T. Akram, M. Abbas, A.I. Ismail, An extended cubic B-spline collocation scheme for time fractional sub-diffusion equation, AIP Conf. Proc. 2184 (1) (2019) 060017.

[38] M. Yaseen, M. Abbas, An efficient computational technique based on cubic trigonometric B-splines for time fractional Burgers' equation, Int. J. Comput. Math. 97 (3) (2020) 725–738.

[39] T. Akram, M. Abbas, M.B. Riaz, A.I. Ismail, N.M. Ali, An efficient numerical technique for solving time fractional Burgers equation, Alex. Eng. J. 2020 (59) (2020) 2201–2220.

[40] G. Fairweather, Spline collocation methods for a class of hyperbolic partial integro-differential equations, SIAM J. Numer. Anal. 31 (2) (1994) 444–460.

[41] L.D. Long, N.H. Luc, S. Tatar, D. Baleanu, N.H. Can, An inverse source problem for pseudo-parabolic equation with Caputo derivative, J. Appl. Math. Comput. 68 (2) (2022) 739–765.

[42] L.D. Long, H.D. Binh, D. Kumar, N.H. Luc, N.H. Can, Stability of fractional order of time nonlinear fractional diffusion equation with Riemann-Liouville derivative, Math. Methods Appl. Sci. 45 (2022) 6194–6216.

[43] T.B. Ngoc, V.V. Tri, Z. Hammouch, N.H. Can, Stability of a class of problems for time-space fractional pseudo-parabolic equation with datum measured at terminal time, Appl. Numer. Math. 167 (2021) 308–329.

[44] L.X. Han, S.J. Liu, An extension of the cubic uniform B-spline curves, J. Comput.-Aided Des. Comput. Graph. 15 (2003) 576–578.

[45] J. Goh, A. Abd. Majid, A.I. Md. Ismail, Extended cubic uniform B-spline for a class of singular boundary value problems, ScienceAsia 37 (2011) 79–82.

[46] C. De Boor, A Practical Guide to Splines, Springer-Verlag, New York, 1978.

[47] I. Wasim, M. Abbas, M.K. Iqbal, A new extended B-spline approximation technique for second order singular boundary value problems arising in physiology, J. Math. Comput. Sci. 19 (2019) 258–267.

[48] S. Sharifi, J. Rashidinia, Numerical solution of hyperbolic telegraph equation by cubic B-spline collocation method, Appl. Math. Comput. 281 (2016) 28–38.

[49] C.A. Hall, On error bounds for spline interpolation, J. Approx. Theory 1 (2) (1968) 209–218.

[50] C. de Boor, On the convergence of odd degree spline interpolation, J. Approx. Theory 1 (4) (1968) 452–463.

[51] S.G. Rubin, R.A. Graves, A Cubic Spline Approximation for Problems in Fluid Mechanics, No. L-9929, 1975.

[52] M. Abbas, A.A. Majid, A.I. Ismail, A. Rashid, The application of cubic trigonometric B-spline to the numerical solution of the hyperbolic problems, Appl. Math. Comput. 239 (2014) 74–88.